Comparison of the effects of two potentials using the Hybrid RMC simulation in BaMn (Fe/V) F_7 glass

S. M. MESLI[a,b*], M. HABCHI[a,b], R. BENALLAL[a,b], M. KOTBI[c].
[a]*École préparatoire en Sciences et Techniques, BP 165 RP Bel Horizon, Tlemcen 13000, Algeria*
[b]*ISP NMSE Division URMER. Belkaid University, BP 119 Tlemcen 13000, Algeria*
[c]*Department of Physics, LPM, A.B. Belkaid University, BP 119 Tlemcen 13000, Algeria*

The $BaMnMF_7$ (M = Fe,V transition metal fluoride glass, assuming isomorphous replacement) have been structurally studied through the simultaneous simulation of their neutron diffraction patterns by a reverse Monte Carlo (RMC) and by the Hybrid Reverse Monte Carlo (HRMC). This last is applied to remedy the problem of the artificial satellite peaks, appear in the partial pair distribution functions (PDFs) by the RMC simulation. The HRMC simulation is an extension of the RMC algorithm, which introduces an energy penalty term (potential) in acceptance criteria. The idea of this paper is to apply the Buckingham potential at the title glass by ignoring the van der Waals terms, in order to make a comparison with the holding into account the van der Waals interactions using combined potential [9]. When displaying the partial pair distribution functions (PDFs), we suggest that the Buckingham potential is more efficient to describe average correlations especially in similar interactions.

(Received August 24, 2015; accepted September 9, 2015)

Keywords: Fluoride glass, RMC and Hybrid RMC simulation, Lennard-Jones potential, Buckingham potential, Partial pair distribution functions.

1. Introduction

Unlike conventional methods, the Reverse Monte Carlo (RMC), based on the experimental data, has the advantage to be applied without any interaction potential model [1,2]. It completes the experiment by computing the pair distribution functions (PDFs) between each two different components of the system. The RMC can be used to simulate different types of ordered and disordered system (liquids, glasses, polymers, crystals and magnetic materials) [3-5]. But the RMC results still display some physically unrealistic aspects, like the appearance of artifacts in PDFs. This can be due to the limited set of experimental data and/or to the non-unique RMC models [6-9]. In order to give realistic feature, we apply a modified simulation protocol based on RMC algorithm, by introducing a physical or chemical constraint based upon the understanding of the material being modelled [10], so we call the Hybrid Reverse Monte Carlo (HRMC) method [6-10].It's also mentioned that the RMC_POT code integrate potential calculation into structural modelling in order to keep molecules together [11].

The $BaMn(Fe,V)F_7$ transition metal Fluoride glasses are among the disordered materials which have been studied through the simultaneous simulation (RMC) [12] and the (HRMC) [9]. The simulation results show that only the 6 first F atom neighbours were constrained around the atoms of Mn and Fe/V, and the octahedra MnF_6, FeF_6, and VF_6 linkage is realized by corner and edge sharing into the $BaMn(Fe,V)F_7$ in crystallized compounds [12]. The barium atom is inserted into the interstice between $[MF_6]$ octahedra.

On the other hand, pair distribution functions (PDFs) between different components of $BaMnFeF_7$ and its fit have been displayed using the HRMC simulation [9], where two types of potentials are combined to build the interaction potential model $U_{ij}^{(1)}$, namely: Coulomb plus Lennard-Jones, which takes into account the van der Waals interactions.

$$U_{ij}^{(1)} = \frac{q_i q_j}{4\pi\varepsilon_0 r_{ij}} + 4\varepsilon \left[\left(\frac{\sigma}{r_{ij}}\right)^{12} - \left(\frac{\sigma}{r_{ij}}\right)^{6}\right] \qquad (1)$$

The purpose of this article is to choose another potential which neglects the dipole-dipole dispersion, in order to perform a comparison of the effects of these two potentials (with and without van der Waals interactions) in $BaMnFeF_7$. So, because it has one less term than Born-Mayer-Huggins potential, simpler to tune and has been used to simulate fluoride glass, the Buckingham potential $U_{ij}^{(2)}$ was selected as the second one [13, 14]. When ignoring the van der Waals interactions, the Buckingham potential is then given as:

$$U_{ij}^{(2)} = \frac{q_i q_j}{4\pi\varepsilon_0 r_{ij}} + A_{ij} exp\left(-\frac{r_{ij}}{\rho_{ij}}\right) \qquad (2)$$

where q_i and q_j are the charges of the individual ions i and j, r_{ij} the atomic distance, ε_0 is the permittivity of free space, A_{ij} is a parameter characterizing the depth of the potential well and ρ is the slope of the short range exponential repulsion and is also known as the hardness parameter [13].The Buckingham potential parameters are selected by fixing the hardness parameters for all the ions [15]. As a first attempt concerning the A_{ij} parameters we have chooses the same depth of the potential well used in the combined potential [9] given by table 1.

Table 1. The Buckingham potential parameters

Pairs	Ba-Ba	Ba-Fe	Ba-Mn	Ba-F	Fe-Fe	Fe-Mn	Fe-F	Mn-Mn	Mn-F	F-F
A_{ij} (eV)	1948.80	10056.50	9956.88	941.30	51897.12	51383.03	4857.58	50874.11	4809.45	454.68
ρ (Å)	0.29	0.29	0.29	0.29	0.29	0.29	0.29	0.29	0.29	0.29

2. Simulation details

The principle of the Reverse Monte Carlo (RMC) simulation is explained in Refs.[1,9], it's a simple tool for constructing large, 3D structural models that are consistent (within the estimated level of their errors) with the total scattering factors obtained from diffraction experiments. Via random movements of particles, the difference (calculated similarly to the χ^2-statistics) between experimental and model total structure factors is minimized. From the particle configurations, the pair distribution functions, as well as other structural characteristics can be calculated [16]. On the other hand, the Hybrid Reverse Monte Carlo (HRMC) simulation is an extension of the RMC algorithm, which introduces an energy penalty term (potential) in acceptance criteria; in order to remedy the problem of the artificial satellite peaks, appear in the partial pair distribution functions (PDFs) by the RMC simulation. For more detailed descriptions of the HRMC method, see Refs [1,7,8,9].

2.1. RMC simulation

Here, we shall only stress the modelling aspect to our system. The present fluoride glass is composed of 5000 atoms (3500 of fluorine; 500 for the rest of each component), put in a cubic box of 20,647 Å length, corresponding to a number density of 0,0710 atoms /Å^3. The initial positions is constituted by a random distribution of Fe, Mn , F and Ba atoms successively, which is limited by the values of the short distance between each atomic pair (cut-off) [9]. In the $BaMnFeF_7$, only the 6 first F atom neighbours were constrained around the atoms of Mn and Fe, and the octahedra [MnF_6],[FeF_6] linkage is realized by corner and edge sharing into the $BaMnFeF_7$ in crystallized compounds [12]. In our case, the initial configuration is constituted by the following geometrical constraints: (1) each Fe atom has six (06) F neighbours between 0 and 2.20 Å; (2) each Mn atom has six (06) F neighbours between 0 and 2.40 Å. While running the RMC code on the title glass, we allow a maximum displacement of 0.08 Å for Ba and Fe, and 0.4 Å for Mn and F.

In our first approach, we fit the RMC simulation total correlation functions to the experimental. The convergence is reached when the difference χ^2 between the calculated and the experimental total distribution functions $G(r_i)$ is minimized. Where $G(r_i)$ is the inverse Fourier transform of the structure factor $S(Q_i)$ depending on the wave vector Q_i.

$$\chi^2 = \sum_i \frac{\left[G^{RMC}(r_i) - G^{EXP}(r_i)\right]^2}{\wp^2(r_i)} \qquad (3)$$

After convergence pair distribution functions PDFs are displayed, by the RMC simulation.

2.2. HRMC simulation

The lack of a potential has the disadvantage that the RMC models have no thermodynamic consistency [17]. The RMC simulation results still display some artificial satellite peaks at the level of PDFs, to remedy this problem, we refer to it as the Hybrid Reverse Monte Carlo simulation. In the HRMC method, we introduce an energy constraint as a potential in addition to the commonly geometrical constraints derived from the experimental data. The agreement factor χ^2 becomes:

$$\chi^2 = \sum_i \frac{\left[G^{RMC}(r_i) - G^{EXP}(r_i)\right]^2}{\wp^2(r_i)} + \frac{\omega U}{k_B T} \qquad (4)$$

Herein U denotes the total potential energy, and ω $(0 < \omega \leq 1)$ is a weighting parameter, it's a statistical weight: which represents the contribution rate of the added potential in the RMC code. The choice of ω value is based on keeping the stability of the system and makes the best fit possible, in this case($\omega = 0.2$). $\wp$ represents the estimated experimental error, which functions as a control parameter for the simulation, in our case($\wp = 0.25$).

So the acceptance criteria expressed by the conditional probability is given as:

$$P_{acc} = exp\left[-\frac{(\chi^2_{new} - \chi^2_{old})}{2}\right] exp\left[-\frac{\Delta U}{k_B T}\right] \qquad (5)$$

$\Delta U = U_{new} - U_{old}$ Is the energy penalty term, U_{new} and U_{old} are the energies of the new and the old configurations, respectively.

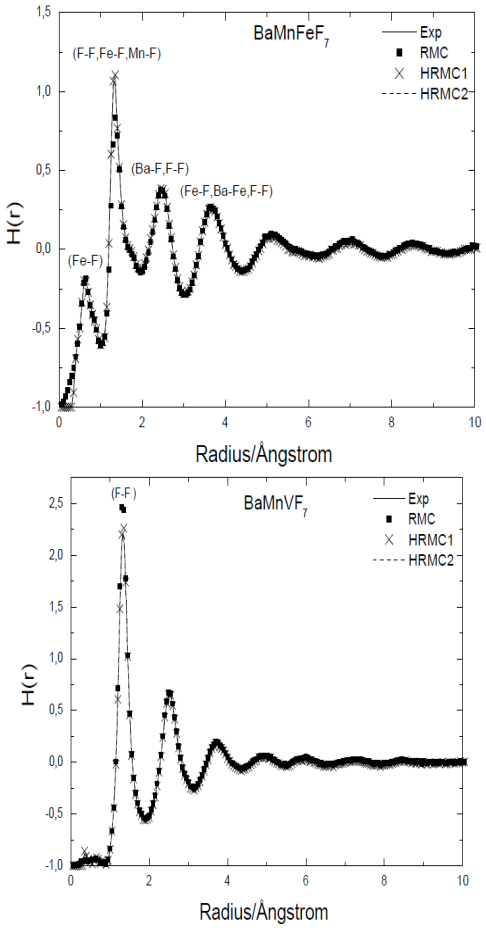

Fig. 1. The experimental total correlation functions $H(r)$ of $BaMnFeF_7$ *and* $BaMnVF_7$ *compared to RMC, HRMC1 and HRMC2 simulations.*

When χ^2 reaches its minimum value, the convergence is attained. The different values of χ^2 are given by table 2. Note that χ_1^2 is the value of the difference between RMC and the experience, χ_2^2 is the value corresponding to the equation 4, with $\left(U = U_{ij}^{(1)}\right)$ derived from HRMC1 simulation, taking the van der Waals interactions into account [9]. And χ_3^2 is the value when $\left(U = U_{ij}^{(2)}\right)$ corresponding to the application of the Buckingham potential, derived from HRMC2 simulation (the present work). Where a better convergence is obtained by HMRC simulation see table 2.

Table 2. χ^2 Values by different simulation, in both structures

χ^2	$BaMnFeF_7$	$BaMnVF_7$
χ_1^2	12.43	9.17
χ_2^2	0.059	0.249
χ_3^2	0.043	0.020

We show the total correlation functions in fig. 1, together with their experimental counterparts. The experimental curves are well fitted. After convergence, we notice that the fluoride glass has preserved its stability after the incorporation of the Buckingham potential, so we can displayed the pair distribution functions by the HRMC simulation in figs. 2 and 3.In order to realize a meaningful comparison of the effects of the two potential (with and without dipole-dipole terms), we keep the same conditions applied to both potentials as: T ,ω, $\wp$, and all of geometrical constraints.

3. Results and discussions

3.1. Total correlation functions: $H(r)$

A comparison with experimental data is of primary importance in order to validate the results of computer simulation methods that use interaction potential models [18]. In this work, the RMC and HRMC code takes into account $G(r)$: the inverse Fourier transform of the total scattering structure factors $S(Q)$. Thus, the quantity used for this purpose is the total distribution function (r) .

Note that it is easy to use total correlation functions equivalent to total distribution functions: $H(r) = G(r) - 1$ see Refs. [7-9]. Fig. 1, provides the simulation total correlation functions for two structures, i.e., $BaMnFeF_7$ and $BaMnVF_7$ compared to the experimental.

Simulation and experimental neutron diffraction results are almost in complete agreement for the two cases. The HRMC2 reproduces well the experience, and preserves the stability of the systems, while maintaining the cohesion of different polyhedra constituting the fluoride glass (MF_6, M = Fe, Mn, V) which show the validity of the choice of the Buckingham potential. And in the first deduction, according to the values of χ^2 table 2, we can conclude a better convergence by applying the Buckingham potential, comparing with the other potential.

The differences of $H(r)$ between the two structures reside in the reduction of average 50% of the intensity of the first peak compared to $BaMnVF_7$, as well as the number in excess of the peaks in the $BaMnFeF_7$. It's the isomorphic substitution (iron / vanadium) which is involved. All vanadium interactions are negligible in $BaMnVF_7$ structure, due to the low diffusion length:$(0.954/-0.03824 \times 10^{-12}$cm, for the pair (Fe/V)) [19].

It is really difficult to distinguish the contributions of pair correlations constructing the total correlation and this especially in the $BaMnFeF_7$ system as four (4) different interactions including iron are added with respect to $BaMnVF_7$. And except in the isomorphic substitution which show that the first peak is corresponding to the specific interaction F-F; due to the high concentration of fluorine and the negligible vanadium interactions. While for $BaMnFeF_7$composition, we refer to the pair distribution functions $g(r)$. And by the same occasion we compare the effect of each potential on the different pair distribution function.

Table 3. Averaged ionic bond length (Å) of similar Interactions by different simulations.

$g(r)$	RMC	HRMC1	HRMC2
F-F	1.350	1.350	1.350
Ba-Ba	3.567	3.550	3.634
Fe-Fe	2.795	2.805	2.791
Mn-Mn	2.690	2.720	2.710

3.2. Pair distribution functions: PDFs

3.2.1 PDFs of similar interactions

For $BaMnFeF_7$ system, ten (10) pair distribution functions $g(r)$ can be displayed by the HRMC simulation. We note that the $g(r)$ including vanadium are also negligible, and the isomorphic substitution (Fe/V) is a technique for better understanding $BaMnFeF_7$ system. One could start with the similar interactions, from where the representation of the PDFs ($g_{XX}(r)$, X = F, Fe, Mn, Ba) figure 2 (a), (b), (c) and (d) respectively. For the (anion-anion) interaction figure 2 (a), peaks for the first, second and third nearest neighbours are clearly appeared to 4 Å by different simulations. This explains the order at short and medium distance in fluoride glasses, which comes from a homogeneous and aperiodic distribution of anions F^-. For the F-F interaction, there is no structural variation observed by all types of simulation. Unlike other interactions, specially on the level of $g_{\mathrm{MnMn}}(r)$ and $g_{\mathrm{BaBa}}(r)$; more realistic futures are given by the HRMC2 compared to the HRMC1, and a good smoothing is observed at the level of the first peak. The ignoring of the dipole-dipole dispersion in $g_{\mathrm{FeFe}}(r)$ is also well marked up to 3.25 Å compared to the to the RMC and HRMC1 results. So the correction given by the Buckingham potential brings more realistic physical structures, and can influence the averaged ionic bond lengths that appear in table 3, which determines the position of the first maximum of the relevant pair distribution functions.

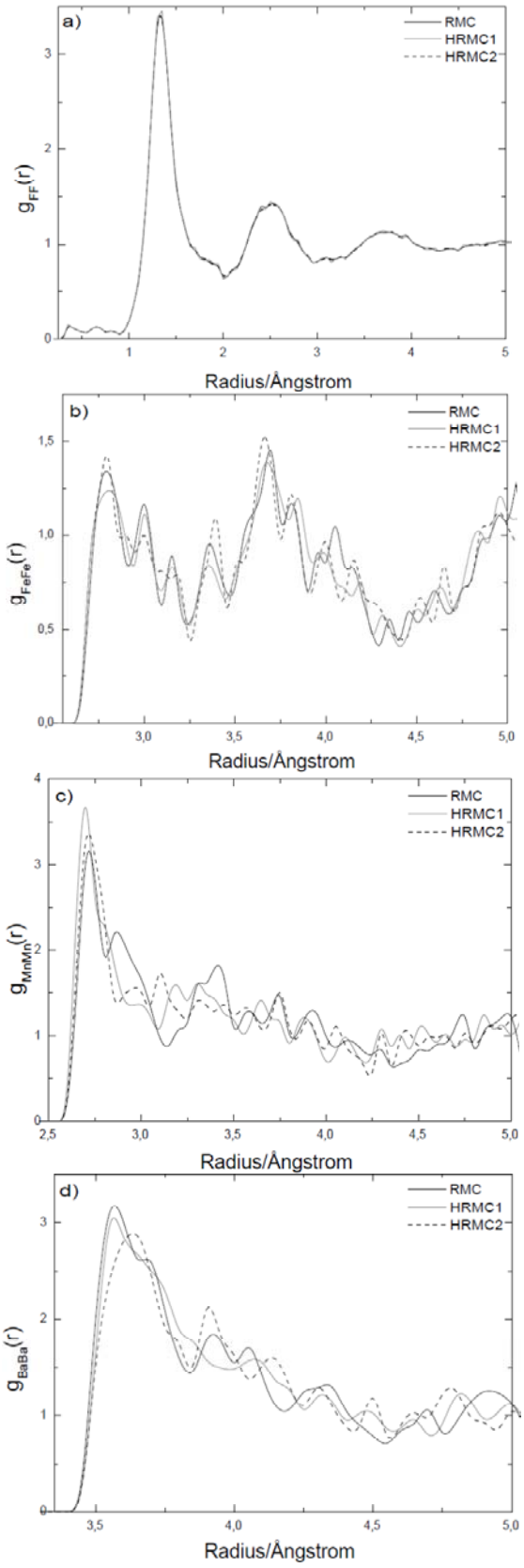

Fig. 2. Pair distribution functions $g(r)$ of similar interactions by RMC , HRMC1 and HRMC2 simulations.

3.2.2 Other PDFs

The distribution of $g_{\mathrm{FeF}}(r)$ is well reproduced by the RMC and by the two potentials consideration. The characteristics below 1 Å are artifacts resulting from Fourier errors or experimental data [9], to do this the first peak around former is between 1.37 and 2.64 Å it's well defined in Fig. 3 (a), which is indicative of a well-ordered local environment. The distribution of $g_{\mathrm{FeF}}(r)$ shows that iron plays the major role in determining the structure. However, for modifiers in figure 3(c), we notice only the appearance of the first peak which is more spatially spread with a lower intensity, which is indicative of a wider distribution of local structures.

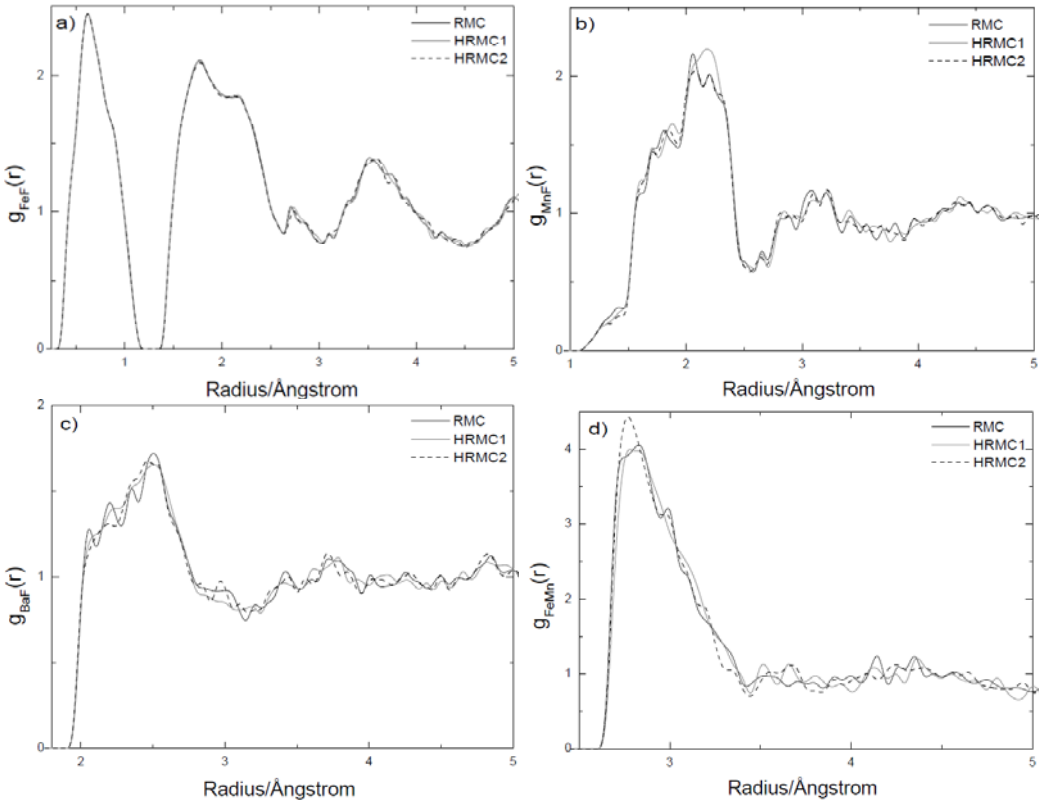

Fig. 3. Pair distribution functions: FeF*(a),* MnF*(b),*BaF *(c) and* FeMn *by RMC, HRMC1 and HRMC2 simulations.*

For the anion-cation interactions like Ba-F and Mn-F, upon comparing the results obtained by HRMC1 and HRMC2, a good smoothing is observed. And comparing with the other interactions, the effect of ignoring the dipole-dipole dispersion of similar interactions is well noticeable. For the Fe-Mn interaction the first peak is well reproduced by HRMC2 simulation, and affects the averaged ionic bond length. The disorder is clearly visible in almost the similar cationic interactions at distances beyond 3 Å in figure 2(b) and 2(c). The different contribution of pair are marked in the total correlation function in figure 1(a) and this is via the different pair distribution functions which is largely dominated by F-F interactions.

Finally, we can deduce that the intervention of the Buckingham potential at the short distance in the in the repulsive interactions is well, compared to the combined potential.

4. Conclusions

In the present work, we perform a comparison of two potential effects applied to the RMC code at $BaMnFeF_7$ fluoride glass. The HRMC1 results take the van der Waals interactions into account, and the HRMC2 when ignoring the dipole-dipole dispersion.

Based on pair distribution functions results we conclude that a good smoothing and a realistic features is obtained using the Buckingham potential specially in the similar interactions at distances which may extend to 3.75 Å. Nevertheless, the others PDFs are also well fitted by the Buckingham potential. Because the application of the added potential kept the stability of the system and there were appreciable improvements in PDFs, the Buckingham potential parameters are accepted.

We can also deduce some structural aspects of transition metal fluoride glass as the vitreous state is coming from the homogeneous distribution of aperiodic anion F^-, and the Fe atoms plays the major role in determining the structure.

Finally, both of potentials play an important role in describing the interactions between atoms of fluoride glass or similar system, promoting the Buckingham potential.

References

[1] R.L McGreevy, L. Pusztai. Mol. Simul. **1,** 359 (1988).
[2] R.L McGreevy, Nucl. Instrum. Meth. A. **1,** 354 (1995).
[3] J.X Zhang, H. Li., J. Zhang, X.G. Song, X.F Bian. Chin. Phys. B **18,** 4949 (2009).
[4] G. Opletal, T.C. Petersen, B O'Malley, I. Snook, D.G.McCulloch, I. Yarovsky, Comput. Phys. Commun.. **178,** 778 (2008).
[5] M.T. Dove, M.G.Tucker, D.A. Keen, Eur. J. Mineral. **14,** 331 (2002)
[6] R. Evans, Mol. Simul. **14,** 409 (1990).
[7] M. Habchi, S.M. Mesli, M. Kotbi, H. Xu, Eur. Phys. J. B. **85,** 255 (2012).
[8] M. Kotbi, H. Xu, M.Habchi, Z. Dembahri, Phys. Lett. A. **315,** 463 (2003).
[9] S.M. Mesli, M. Habchi, M. Kotbi, H. Xu. Condens. Matter. Phys. **16,** 1-8 (2013).
[10] K.S. Jain, R.J.-M. Pellenq, J.P. Pikunic, K.E. Gubbins, Langmuir. **22,** 9942 (2006).
[11] O. Gereben, L. Pusztai, J. Comput. Chem. **33,** 2285 (2012).
[12] A. Le Bail, Reverse Monte Carlo and Rietveld Modelling of $BaMn(Fe/V)F_7$ structures from neutron data, Proceeding of CONCIM -April 2003, Bonn Germany.
[13] S. Gruenhut, MacFarlane, R. Douglas, J. Non-Cryst. Solids. **184,** 356-362 (1995).
[14] S.Gruenhut., M. Amini, MacFarlane, R Douglas, P Meakin, J. Non-Cryst. Solids. **213,** 398 (1997) .
[15] J. Lucas, C.A Angell, S. Tamaddon, Mater.Res.Bull Non-Cryst. **19,** 945 (1984).
[16] O. Gereben, P.Jovari, L.Temleitner, L.Pusztai, J. Optoelectron. Adv. Mater **9,** 3021 (2007)
[17] R. L. McGreevy, J. Phys. Condens. Matter. **13,** R877. (2001).
[18] L. Pusztai, I. Hars\'anyi, H. Dominguez, O. Pizio, Chem. Phys. Letts. **457,** 96 (2008).
[19] A. Le Bail, J. Non-Cryst. Solids. **271,** 249 (2000).

[*]Corresponding author: msidim1975@gmail.com